

Erasable Nanoporous Antireflection Coatings Based on the Reconstruction Effect of Layered Double Hydroxides**

Jingbin Han, Yibo Dou, Min Wei,* David G. Evans, and Xue Duan

Antireflection coatings play a pivotal role in photovoltaic and display devices and all kinds of optical lenses,^[1] because they can effectively reduce the intensity of reflected light at interfaces, which translates into increased transmission, improved contrast, reduced glare, and the elimination of ghost images. The principle of antireflection (AR) coatings is based on the destructive interference of reflected light from air–film and film–substrate interfaces. An ideal homogeneous single-layer AR coating satisfies the following conditions:^[2] 1) The thickness of the coating is $\lambda/4$, where λ is the wavelength of the incident light; and 2) $n_c = (n_a n_s)^{1/2}$, where n_c , n_a , and n_s are the refractive indices of the coating, air, and the substrate, respectively. To satisfy these prerequisites for an effective AR coating on glass or plastics ($n_a = 1$ and $n_s = 1.5$), n_c should be 1.22. Although condition (1) can be easily met, condition (2) imposes a problem, as natural materials with such a low refractive index are either rare or expensive to obtain in thin-film form. One effective solution to this problem is to use appropriately designed porous materials,^[3] because the introduction of the nanopores can reduce the refractive index of the coatings and achieve the AR requirement.

In recent years, many methods have been developed to obtain nanoporous film materials for use as AR coatings, including sol–gel processes,^[4] phase-separation,^[5] a sacrificial porogen approach,^[6] layer-by-layer (LBL) deposition of nanoparticle multilayers,^[7] plasma-enhanced chemical vapor deposition,^[8] and deposition of nanorods or nanowires.^[9] In particular, these nanoporous films with low refractive indices (n_c) and thickness in the range 80–220 nm (about one-quarter of the range of visible wavelengths) can be applied as efficient antireflection coatings to improve the light transmission of transparent substrates in the visible wavelength range. However, only a few reports have focused on intelligent AR coatings. For example, Rubner and co-workers reported an intelligent multilayer polymer film with a nanoporous structure that could be erased and reconstructed by cycling


solution pH, which endowed the film with reversible AR properties.^[10] However, polymer-based materials generally exhibit low optical and thermal stability and also environmental incompatibility, which restricts their long-term application.

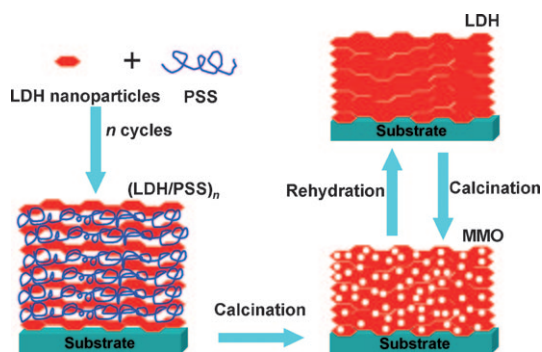
Layered double hydroxides (LDH) are layered anionic clays that are generally expressed by the formula $[M^{2+}_{1-x}M^{3+}_x(OH)_2](A^{n-})_{x/n} \cdot mH_2O$, where M^{2+} and M^{3+} are di- and trivalent metal cations, and A^{n-} is a counteranion.^[11] The host structure consists of brucite-like layers of edge-sharing $M(OH)_6$ octahedra, and the partial substitution of M^{3+} for M^{2+} results in positively-charged host layers, which are balanced by the interlayer anions.^[12] One of the most exploited properties of LDH materials is the so called “reconstruction effect”.^[13] calcination of LDHs at moderate temperatures leads to the formation of mixed metal oxides (MMO) with a porous structure, and rehydration of MMO results in spontaneous structural reconstruction of the LDH. The fabrication of porous MMO materials using a sacrificial template method has been reported by Prévot et al.^[14] Recently, Lu et al.^[15] reported the observation of colloidal LDH nanoparticle suspensions in aqueous solution with a positive zeta potential in the range 30–50 mV. This zeta potential indicates that the external surface of LDH nanoparticles is positively charged, even though most of the positive charges of the LDH host layers are neutralized by interlayer species. Therefore, colloidal LDH nanoparticles can be regarded as ideal building blocks without any surface modification for the assembly of functional multilayer films with negatively charged electrolytes by the electrostatic LBL technique.

Herein, we present an erasable nanoporous AR coating based on the reconstruction effect of LDH materials. The precursor films were fabricated by assembly of LDH nanoparticles with the polyanion poly(sodium styrene-4-sulfonate), denoted as PSS, by an electrostatic LBL method, yielding the LDH/PSS multilayer films. Then nanoporous films with AR properties were obtained by calcination of LDH/PSS films by utilizing the so-called sacrificial porogen (pore generator) approach: The selective removal of the porogen (PSS and the interlayer anions of LDH) results in the formation of MMO films with a nanoporous structure (Scheme 1). This versatile process is particularly amenable to the creation of large-area uniform AR coatings on non-flat surfaces with precise control over thickness and optical properties. More significantly, after rehydration of the MMO films, the transformation to the non-porous LDH structure can be achieved by the structural “reconstruction effect” of LDH materials. By cycling the calcination–rehydration process, the AR properties of the coating can be

[*] J. Han, Y. Dou, Prof. M. Wei, Prof. D. G. Evans, Prof. X. Duan
State Key Laboratory of Chemical Resource Engineering, Beijing
University of Chemical Technology
Box 98, Beijing 100029 (P.R. China)
Fax: (+86) 10-6442-5385
E-mail: weimin@mail.buct.edu.cn

[**] This work was supported by the National Natural Science Foundation of China, the Chinese Universities Scientific Fund (Grant No.: ZZ0908), the 111 Project (Grant No.: B07004), and the 973 Program (Grant No.: 2009CB939802).

 Supporting information for this article, including preparative details and characterization, is available on the WWW under <http://dx.doi.org/10.1002/anie.200907005>.



Scheme 1. Fabrication of erasable antireflection coatings based on the reconstruction effect of layered double hydroxides (LDHs). MMO: mixed metal oxide, PSS = poly(sodium styrene-4-sulfonate).

switched on and off between porous and non-porous states. To the best of our knowledge, there has been no prior report of erasable AR coatings based on inorganic films.

The suspension of colloidal MgAl-LDH nanoparticles was obtained by using a method that involves separate nucleation and aging steps (SNAS),^[16] in which rapid mixing and nucleation in a colloid mill is followed by a separate aging process. The X-ray diffraction (XRD) pattern (Supporting Information, Figure S1) and FTIR spectrum (Supporting Information, Figure S2) of the MgAl-LDH powder sample indicate a well-defined nitro-LDH (NO_3 -LDH) with high crystallinity. The scanning electron microscopy (SEM) image (Supporting Information, Figure S3) reveals that the individual MgAl- NO_3 LDH nanoplatelets with particle size of 80–100 nm and an aspect ratio of 6–8 crystallized with a narrow size distribution. Elemental analysis shows that the molar ratio of Mg/Al is close to 2:1 and the Al/N ratio close to 1:1, as expected. The well-dispersed suspension was transparent and stable without any precipitation when stored in an N_2 atmosphere for more than one month.

The subsequent growth of LDH/PSS multilayer film was monitored by means of the UV/Vis absorption bands of PSS (193 and 225 nm) as depicted in Figure 1. The LBL assembly

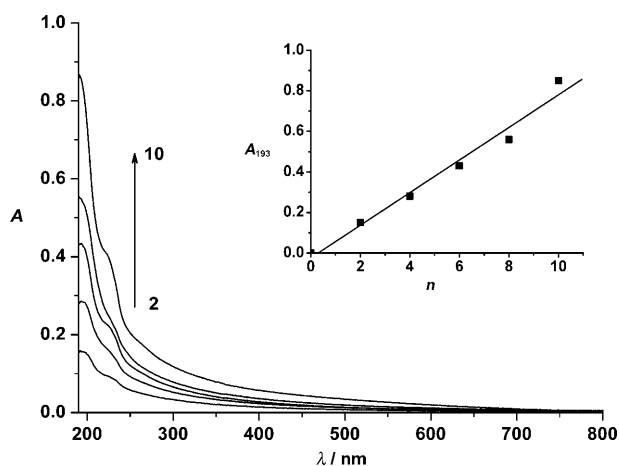


Figure 1. UV/Vis absorption spectra of $(\text{MgAl-LDH/PSS})_n$ films ($n=2$ –10) assembled on quartz glass substrates. Inset: Absorbance at 193 nm A_{193} plotted against the bilayer number n .

process is driven by electrostatic interactions between the positively charged LDH nanoparticles and the negatively charged PSS. A linear increase in absorbance at 193 nm was observed upon increasing the number of bilayers (Figure 1, inset), which indicates a stepwise and regular deposition of LDH nanoparticle/PSS multilayer films. The thickness of the LDH/PSS films determined by cross-sectional SEM images (Figure 2 a–c) increased with an average increment of about 29 nm per deposition cycle. After calcination of the LDH/PSS film at 450 °C for 3 h, the film thickness decreased dramatically (ca. 35 %), and the cross-sectional SEM images show that the original impacted LDH nanoplatelets transform to loosely stacked nanoparticles with a porous structure (Figure 2 c,d). The phase transformation from LDH to mixed metal oxides (MMO) during the calcination process was confirmed by XRD. The as-prepared $(\text{LDH/PSS})_{10}$ film displays a characteristic 003 reflection of NO_3 -LDH (Figure 3 a) with a basal spacing of 8.73 Å. Calcination at 450 °C gives rise to the appearance of reflections (200 and 220) of a MgO phase (periclase; Figure 3 b).^[17]

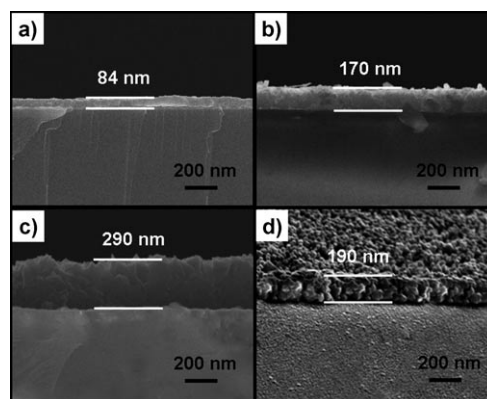


Figure 2. Cross-sectional SEM images of $(\text{LDH/PSS})_n$ films with a) $n=3$, b) $n=6$, c) $n=10$, and d) an MMO film obtained by calcination of (c).

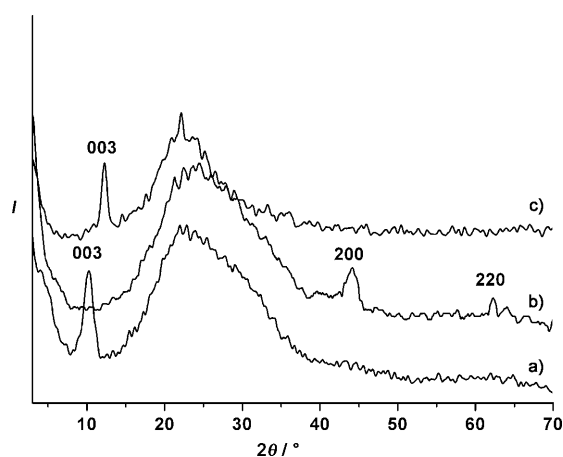


Figure 3. XRD patterns of a) the $(\text{LDH/PSS})_{10}$ film, b) the MMO_{10} film obtained by calcination of (a), and c) the rehydrated LDH film obtained by hydrothermal treatment of (b).

The AR properties of the MMO_n films on quartz substrates (n is the number of deposition cycles of the corresponding precursor LDH/PSS film) were investigated by using the transmission spectra (Figure 4). The transmission

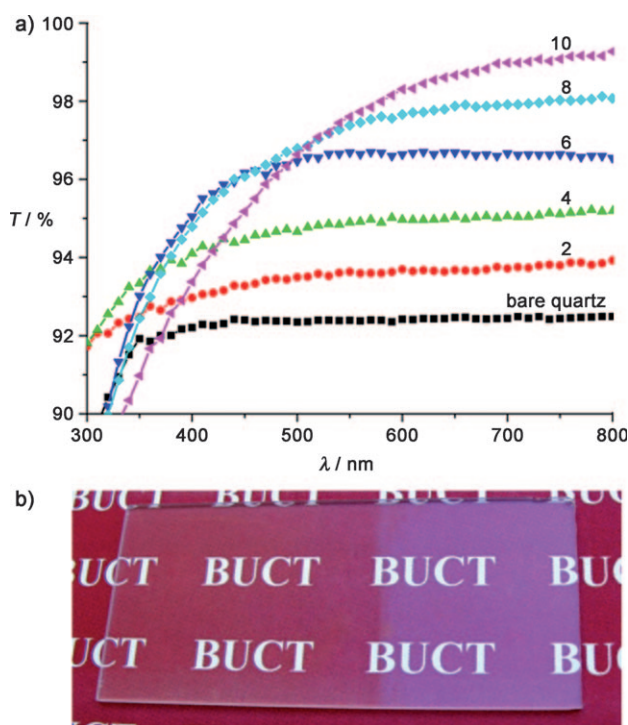


Figure 4. a) Transmittance spectra of MMO_n films ($n=0, 2, 4, 6, 8$, and 10) deposited on quartz substrates. b) Photograph of a quartz substrate exposed to sunlight. The left portion has been coated with MMO_{10} .

spectrum of bare quartz is also provided for comparison, with a transmittance of about 92% in the spectral range 350–800 nm. The transmittance increased significantly for the MMO_n film-coated quartz substrates. The transmittance of MMO_n films in visible region was readily tuned by changing the coating thickness, which can be achieved by simply varying the bilayer number of the precursor film. For a MMO_{10} film, a transmittance of 98.6% was obtained at a wavelength of 650 nm. The AR properties of the MMO film are also readily apparent in Figure 4b. The letters below the quartz with the AR coating (left side) are much clearer than those below bare quartz (right side), demonstrating the increased transparency and reduced reflection of the MMO -coated quartz slide.

The AR properties of the MMO_n films can be erased by a rehydration process. Figure 5 shows the reversible erasure–regeneration cycles of the AR properties of MMO_{10} film. When the MMO_{10} film (1) was rehydrated by hydrothermal treatment, reflective loss was observed and it no longer acted as an AR coating (2); the AR properties were restored by further calcination (3). Reversible switching between AR and non-AR films over several cycles is reproducible by alternate processes of calcination and rehydration (Figure 5, inset).

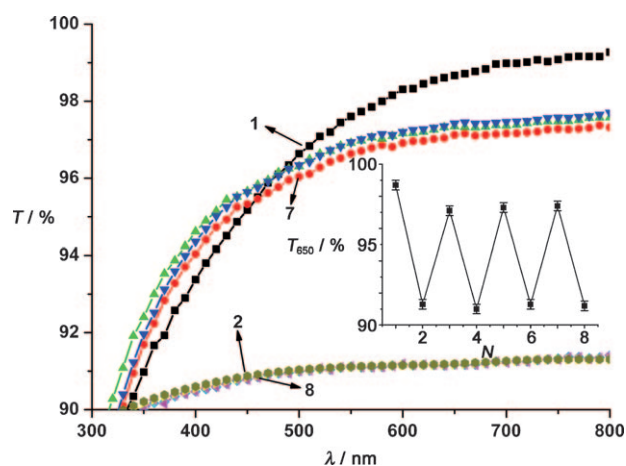


Figure 5. UV/Vis transmittance spectra of the MMO_{10} film (1, 3, 5, 7) and the rehydrated LDH film (2, 4, 6, 8). The inset shows the transmittance at 650 nm T_{650} as a function of cycle number N ; cycling occurs between MMO and LDH films.

SEM was used to observe the change in film morphology for one AR and non-AR film. The as-prepared $(\text{LDH/PSS})_{10}$ film (Figure 6a) shows a compact and dense accumulation of

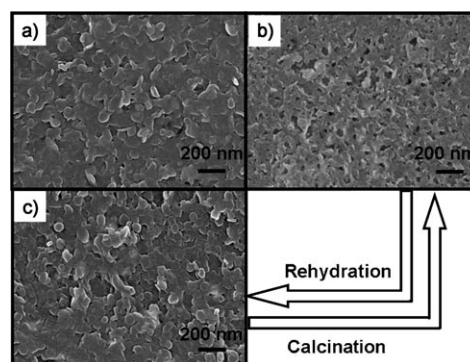


Figure 6. SEM images of a) the $(\text{LDH/PSS})_{10}$ film, b) the MMO_{10} film obtained by calcining (a), and c) the rehydrated LDH film obtained by hydrothermal treatment of (b).

LDH platelets with particle size in the range 80–100 nm; in contrast, the MMO_{10} film (Figure 6b) has a highly porous structure, with a pore size of 20–40 nm, resulting from the removal of porogen species. After rehydration, the film recovers its originally dense (non-porous) morphology (Figure 6c). The structure of the rehydrated MMO film investigated by XRD (Figure 3c) reveals a (003) reflection of an LDH phase with basal spacing of 7.21 Å, which corresponds to an hydroxy-containing LDH.^[18] This indicates that the original NO_3 -LDH (with basal spacing of 8.73 Å) transformed to OH-LDH after an erasure–regeneration cycle. Both the XRD and SEM results demonstrate that the calcination–rehydration cycle induces the conversion between nanoporous MMO films and compact LDH films, which endows the films with erasable AR properties.

Long-term stability is extremely important for the practical application of AR coatings. The AR properties did not show any decrease after storage of the porous MMO films under ambient conditions for 120 days, thus demonstrating the excellent stability of these AR coatings. The mechanical stability was examined by sonicating the quartz substrate coated with MMO_n film in water containing a detergent. After 1 h of sonication in a sonicator (100 W), the AR properties remained unchanged. Furthermore, the adhesion of the coatings to the substrate was also examined by a standard adhesive tape peel test, and the AR properties showed no change after peeling of the tape (Supporting Information, Figure S4). During the fabrication of the AR coatings, the removal of porogen components (PSS and interlayer anions) by calcination leads to an inorganic coating with a cross-linked porous framework, which greatly improves the mechanical stability and adhesion to substrates, and guarantees the long-term application of the AR coatings under practical conditions.

In summary, we have presented a facile and cost-effective method for the fabrication of AR coatings by LBL deposition of LDH nanoparticles with PSS on quartz substrates, followed by calcination. The resulting MMO_n films exhibit tunable optical properties as a function of film thickness, and a transmittance above 98% was obtained at 650 nm for the MMO₁₀ film. Moreover, the AR properties can be switched on and off between the porous (MMO film) and non-porous state (LDH film) by the reconstruction effect of LDH materials through recycling the calcination–rehydration procedure, which makes the MMO_n film an effective candidate for erasable AR coatings. Therefore, this work provides a novel approach to fabricate inorganic intelligent AR films with high mechanical stability, strong adhesion to substrates and environmental friendliness for viable long-term application.

Received: December 12, 2009

Published online: February 19, 2010

Keywords: coatings · erasing · layer-by-layer assembly · layered double hydroxides · nanostructures

- [1] a) Y.-J. Lee, D. S. Ruby, D. W. Peters, B. B. McKenzie, J. W. P. Hsu, *Nano Lett.* **2008**, *8*, 1501; b) S. Walheim, E. Schäffer, J. Mlynek, U. Steiner, *Science* **1999**, *283*, 520; c) P. Yu, C.-H. Chang,

- C.-H. Chiu, C.-S. Yang, J.-C. Yu, H.-C. Kuo, S.-H. Hsu, Y.-C. Chang, *Adv. Mater.* **2009**, *21*, 1618.
 [2] H. A. Macleod, *Thin-Film Optical Filters*, Elsevier, New York, **1969**.
 [3] a) J. Cho, J. Hong, K. Char, F. Caruso, *J. Am. Chem. Soc.* **2006**, *128*, 9935; b) Z. Gemici, P. I. Schwachulla, E. H. Williamson, M. F. Rubner, R. E. Cohen, *Nano Lett.* **2009**, *9*, 1064.
 [4] A.-L. Pénard, T. Gacoin, J.-P. Boilot, *Acc. Chem. Res.* **2007**, *40*, 895.
 [5] a) M. Ibn-Elhaj, M. Schadt, *Nature* **2001**, *410*, 796; b) C.-Y. Kuo, Y.-Y. Chen, S.-Y. Lu, *ACS Appl. Mater. Interfaces* **2009**, *1*, 72.
 [6] a) H.-C. Kim, J. B. Wilds, C. R. Kreller, W. Volksen, P. J. Brock, V. Y. Lee, T. Magbitang, J. L. Hedrick, C. J. Hawker, R. D. Miller, *Adv. Mater.* **2002**, *14*, 1637; b) L. B. Zhang, Y. Li, J. Q. Sun, J. C. Shen, *Langmuir* **2008**, *24*, 10851; c) G.-D. Fu, Z. Yuan, E.-T. Kang, K.-G. Neoh, D. M. Lai, A. C. H. Huan, *Adv. Funct. Mater.* **2005**, *15*, 315.
 [7] a) Y. Li, F. Liu, J. Q. Sun, *Chem. Commun.* **2009**, 2730; b) D. Lee, M. F. Rubner, R. E. Cohen, *Nano Lett.* **2006**, *6*, 2305.
 [8] L. Martinu, D. Poitras, *J. Vac. Sci. Technol. A* **2000**, *18*, 2619.
 [9] a) S. L. Diedenhofen, G. Vecchi, R. E. Algra, A. Hartsuiker, O. L. Muskens, G. Immink, E. P. A. M. Bakkers, W. L. Vos, J. G. Rivas, *Adv. Mater.* **2009**, *21*, 973; b) J.-Q. Xi, J. K. Kim, E. F. Schubert, *Nano Lett.* **2005**, *5*, 1385.
 [10] J. Hiller, J. D. Mendelsohn, M. F. Rubner, *Nat. Mater.* **2002**, *1*, 59.
 [11] a) Z. P. Xu, P. S. Braterman, *J. Phys. Chem. C* **2007**, *111*, 4021; b) G. R. Williams, D. O'Hare, *J. Mater. Chem.* **2006**, *16*, 3065; c) L. Li, Y. Feng, Y. Li, W. Zhao, J. Shi, *Angew. Chem.* **2009**, *121*, 6002; *Angew. Chem. Int. Ed.* **2009**, *48*, 5888; d) Z. P. Xu, P. S. Braterman, K. Yu, H. F. Xu, Y. F. Wang, C. J. Brinker, *Chem. Mater.* **2004**, *16*, 2750.
 [12] a) R. Ma, K. Takada, K. Fukuda, N. Iyi, Y. Bando, T. Sasaki, *Angew. Chem.* **2008**, *120*, 92; *Angew. Chem. Int. Ed.* **2008**, *47*, 86; b) M. Darder, M. L. Blanco, P. Aranda, F. Leroux, *Chem. Mater.* **2005**, *17*, 1969; c) L. Desigaux, M. B. Belkacem, P. Richard, J. Cellier, P. Léone, L. Cario, F. Leroux, C. Taviot-Guého, B. Pitard, *Nano Lett.* **2006**, *6*, 199; d) K. Ebitani, K. Motokura, T. Mizugaki, K. Kaneda, *Angew. Chem.* **2005**, *117*, 3489; *Angew. Chem. Int. Ed.* **2005**, *44*, 3423.
 [13] a) F. Millange, R. I. Walton, D. O'Hare, *J. Mater. Chem.* **2000**, *10*, 1713; b) J. Rocha, M. del Arco, V. Rives, M. A. Ulibarri, *J. Mater. Chem.* **1999**, *9*, 2499.
 [14] E. Géraud, V. Prévot, J. Ghanbaja, F. Leroux, *Chem. Mater.* **2006**, *18*, 238.
 [15] Z. P. Xu, G. S. Stevenson, C. Q. Lu, G. Q. Lu, P. F. Bartlett, P. P. Gray, *J. Am. Chem. Soc.* **2006**, *128*, 36.
 [16] Y. Zhao, F. Li, R. Zhang, D. G. Evans, X. Duan, *Chem. Mater.* **2002**, *14*, 4286.
 [17] O. D. Pavel, R. Birjega, M. Che, G. Costentin, E. Angelescu, S. Serban, *Catal. Commun.* **2008**, *9*, 1974.
 [18] M. J. Climent, A. Corma, S. Iborra, A. Velty, *J. Catal.* **2004**, *221*, 474.